IUST
Iran University of Science and Technology

Iranian Journal of Electrical and Electronic Engineering

Journal Homepage: ijeee.iust.ac.ir

Online-Tuning Fuzzy Logic Controller Based Particle Swarm Optimization Proportional-Integral (FLC-PSO-PI) For Multilevel Inverter of Output Voltage Regulation

Ying Foo Leong*, Nizaruddin M. Nasir*, Suliana Ab-Ghani*, Norazila Jaalam* and Nur Huda Ramlan*(C.A.)

Abstract: This paper focuses on the application of a cascaded multilevel inverter, specifically the 5-level multilevel inverter, utilizing a proposed controller known as the FLC-PSO-PI controller. The primary challenge addressed in this research is the precise regulation of output voltage in the multilevel inverter during load variations while meeting voltage harmonic and transition requirements as per industry standards, which are the 10 % voltage limit recommended by IEC and 8 % of total harmonic distortion (THD) by IEEE. An innovative solution is proposed by integrating PSO and FLC to dynamically adapt the controller in real-time, ensuring stable and accurate output voltage regulation. The proposed controller is designed and simulated using MATLAB/Simulink, and its performance is compared with PSO-PI and no controller under various load conditions. The results demonstrate that the FLC-PSO-PI controller significantly enhances output voltage regulation were achieving the desired peak voltage and low THD across different load scenarios, including half load to full load (0.8 %) and no load to full load (0.89 %). Furthermore, the FLC-PSO-PI controller exhibits superior transient response characteristics, such as reduced overshooting (2.89 %), faster rise time at 36.946 µs, and satisfactory settling time at 151.014 µs. This research contributes to the advancement of multilevel inverter technology and its potential applications in renewable energy systems, motor drives, and grid-connected devices. The proposed FLC-PSO-PI controller offers a promising solution for precise voltage regulation in multilevel inverters, enhancing their performance and enabling widespread adoption in various industrial sectors.

Keywords: Cascaded H-Bridge Multilevel Inverter (CHMI), Proportional-Integral (PI), Particle Swarm Optimization (PSO), Fuzzy Logic Controller (FLC)

1 Introduction

IN recent years, multilevel inverter (MLI) has garnered significant interest among researchers [1], [2]. MLIs utilize cascading voltages from multiple DC sources to generate a stepped-up voltage waveform [3], [4]. The voltage distribution across the switches in the MLI occurs at various levels, leading to reduced voltage derivatives. This reduction in the derivative characteristic also directly decreases electromagnetic interference, contributing to an improvement in power quality. The multiple output produced by the MLI also help in reducing the overall THD in the output voltage waveform [5], [6]. This enhanced capability of the MLI in the inverter provides more control over voltage and current. One of the variations of the multilevel inverter is the cascaded H-bridge multilevel inverter (CHMI).

In electrical systems, precise voltage control is crucial due to the inverse relationship between voltage and current [7], [8]. Higher current draw leads to increased voltage drop. Variations in load result in changes on current draw, impacting the voltage drop. Voltage drops

Iranian Journal of Electrical & Electronic Engineering, 2025.
Paper first received 17 Dec 2024 and accepted 22 Feb 2025.
* The author is with the Faculty of Electrical and Electronics Engineering Technology, Universiti Malaysia Pahang Al-Sultan Abdullah, 26600 Pekan, Pahang, Malaysia.
E-mails: yingfoo55@gmail.com, n99zrd@gmail.com, suliana@umpsa.edu.my, zila@umpsa.edu.my, hudaramlan@umpsa.edu.my.
Corresponding Author: Nur Huda Ramlan.

can potentially damage electrical equipment [9]. Therefore, regulating the output voltage of a CHMI is crucial for ensuring high power quality. The IEEE 519 standard recommends keeping THD below 8 % when voltage less than 1 kV [10], while the IEC 60038 standard sets a voltage limit of ± 10 % [11].

To ensure voltage regulation, a controller is utilized. The use of a proportional-integral (PI) controller is commonly adopted for multilevel inverters like CHMI due to its simple structure, high stability, minimal steady-state error, and ease of implementation [12]. However, it has limitations such as slow response, high overshoot, sensitivity to gains, and sluggish reaction to disturbances [13]. To address these issues, optimization techniques like particle swarm optimization (PSO) can be applied to fine-tune the PI controller parameters. The work has been done in [14], [15], [16] that applies this methodology in dual active bridge converter that resulted in faster response and high accuracy. While [17] applies in hybrid multilevel inverter that resulted in strengthen voltage regulation and maintaining low level of THD. Furthermore, employing an online tuning method like a fuzzy logic controller (FLC), known for its data-driven approach, become a preferred option for managing nonlinearity effectively over extended durations. The hybridization of FLC, PSO and PI concepts emerged from the need for a controller that can be optimized online in real-time. Traditional PSO-PI controllers require manual tuning of PI parameters [18], which it can be automatically adjusted to achieve optimal performance. Researchers [19] shows excellent performance of Fuzzy-PSO-PI controller applied to motor drive under various load condition. On the other hand, based on their research [20], [21] shows that this hybrid controller also performs well in renewable energy application. Existing literature does not seem to extensively cover the study of this proposed controller in the context of multilevel inverter output voltage regulation.

2 Methodology

2.1 Five-level MLI

The 5-level CHMI is constructed by interconnecting two H-bridge inverters consist of 8 IGBT (insulated-gate bipolar transistor) switches to separate dc sources in series [22], as depicted in Fig. 1. This configuration results in various switching states within the inverter. The switching sequence was created using the Sinusoidal Pulse Width Modulation (SPWM) technique that specifically in the level shifting of phase opposition disposition. After that, the inverter is linked to a low-pass filter that smoothens the staircase waveform generated by the inverter into a sinusoidal waveform. Thus, the filtered waveform is directed to the load for utilization. The specifications of the multilevel inverter used in the simulation are detailed in Table 1.

Table 1. Multilevel inverter simulation parameters.

Parameter	Value
DC Voltage Source, V_{DC}	2 × 100 V
System frequency, f	50 Hz
Switching frequency, f_{sw}	50 kHz

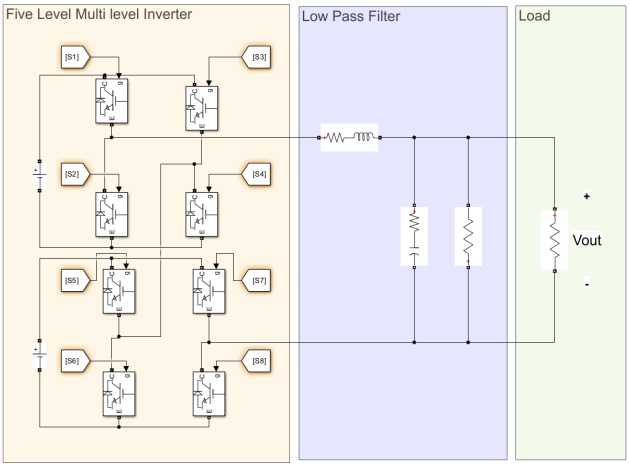

Fig 1. Five-level CHMI.

2.2 Double loop PI controller based on PSO algorithm

- **Dynamic model of multilevel inverter**

The integration of various multilevel inverter configurations, encompassing different structure in power switches bridge and the utilization of bipolar or unipolar modulation tailored for single-phase inverter. The equivalent circuit is symbolized by the filter of the inverter.

Table 2. Low pass filter parameters.

Parameter	Value
Output voltage, V_o	180 V
Cut-off frequency, f_{cutoff}	5 kHz
Resistor, R	8.1 Ω
Inductor, L	0.3646 mH
Capacitor, C	2.77875 µF

All the LC low pass filter parameters recorded in Table 2. The equivalent circuit can be further modelled in a block diagram model as in Fig. 2. In this diagram, the output voltage, inductor voltage and inverter input are represented as V_O, V_L, and V_{in}, respectively. The transfer function of the filter denoted as "FirstLoop(s)" is defined in given Eq. (1).

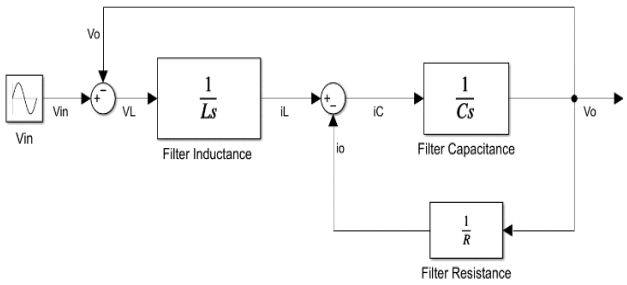

Fig 2. Block diagram of inverter's filter model.

$$FirstLoop(s) = \frac{V_o(s)}{V_L(s)} = \frac{R}{RLCs^2+Ls+R} \quad (1)$$

- **Double-loop PI controller**

In the double-loop PI controller structure, the output voltage (V_o) and inductor current (i_L) are utilized and compared with the reference signal of output voltage and inductor current. Hence, two PI controllers are implemented based on these parameters. The transfer function for both controllers is represented by Eq. (2) and Eq. (3), where the state space model of the voltage controller is denoted as "VoltageCont(s)" and the current controller as "CurrentCont(s)", respectively. The proportional gain and integral for the voltage controller are labelled as "Vk_p" and "Vk_i", respectively, while for the current controller, they are ""Ik_p" and "Ik_i". These four variables serve as distinct values that can be determined using metaheuristic optimization.

$$VoltageCont(s) = Vk_p + \frac{Vk_i}{s} \quad (2)$$

$$CurrentCont(s) = Ik_p + \frac{Ik_i}{s} \quad (3)$$

In theory, the error of the voltage control will be adjusted to generate a reference signal of the inductor current. This reference signal will be compared with "i_L" and processed in the current controller. Moreover, a control signal for PWM control of the inverter will be derived from these controllers and utilized as the switching signal for the power switches. The equivalent block diagram model representing this process is depicted Fig. 3.

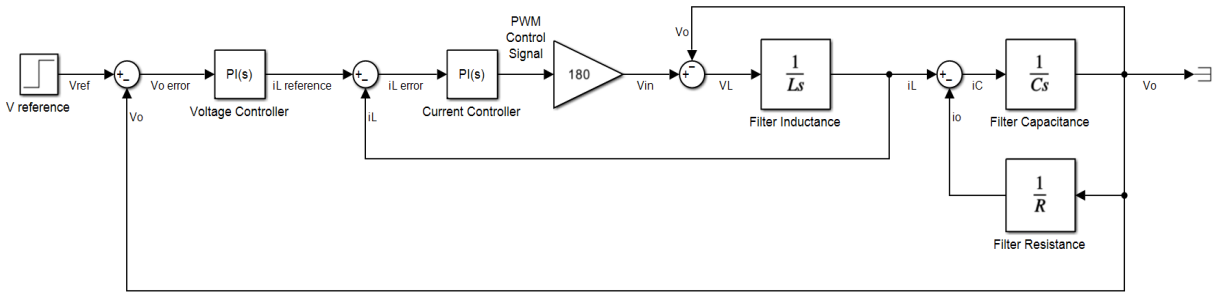

Fig 3. Double loop closed loop system.

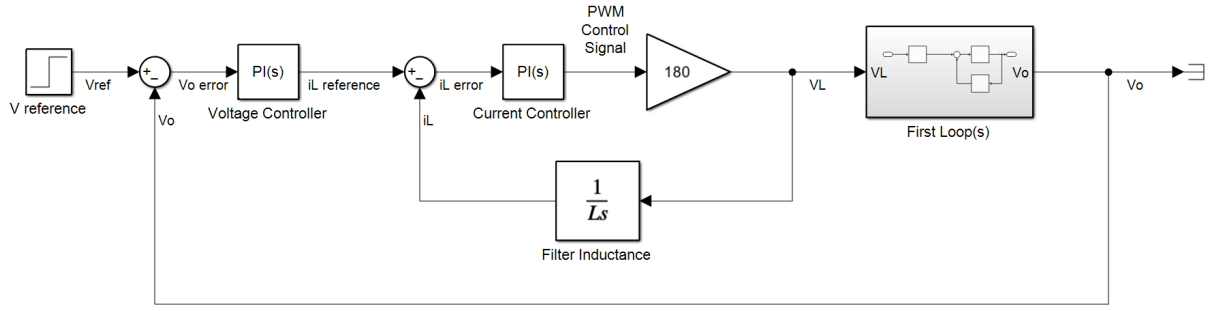

Fig 4. Second looping block diagram.

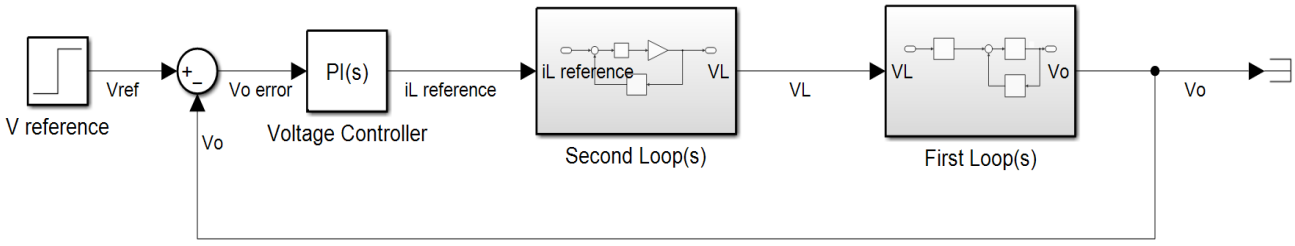

Fig 5. Entire inverter system.

The transfer function to create a dynamic model for this system can be derived by considering the number of looping in the block diagram system. The first looping is established based on the state space model of the inverter's filter, as described in Eq. (1). Following the creation of the first loop, the second looping of this system is formed using the block diagram reduction method, incorporating feedback from the filter inductor. Fig. 4 illustrates the construction of the second loop through block diagram reduction. Equation (4) presents the mathematical model of the transfer function for the second loop.

$$Secondloop(s) = \frac{C(s)}{R(s)} = \frac{G(s)}{1+G(s)H(s)} = \frac{CurrentCont(s)}{1+CurrentCont(s)*\frac{1}{Ls}} \quad (4)$$

The block reduction method of this process leaves the entire block diagram as Fig. 5.

Hence, the overall transfer function denoted as "InverterSystem(s)" that can be utilized as a model-based controller is represented by Eq. (5).

$$InverterSystem(s) = \frac{VoltageCont(s)*First\ loop(s)*\ Second\ loop(s)}{1+VoltageCont(s)*First\ loop(s)*\ Second\ loop(s)} \quad (5)$$

The dynamic model represented by Eq. (5) is implemented in a MATLAB syntax script. In this script, a metaheuristic approach, specifically the PSO algorithm is utilized to determine the values of the four parameters: Vk_p, Vk_i, Ik_p, and Ik_i.

- **Model based PSO**

The MATLAB software executes the PSO algorithm iteratively until it converges to the best fitness, which corresponds to the lowest error from objective function within the expected range of boundaries. The PSO algorithm properties such as particle swam size is 10, maximum iteration is 100 and total number of variables is 4. The lower bound and upper bound of PI parameters value for each voltage controller and current controller in PSO algorithm setting are recorded in Table 3.

Table 3. Bound value of PI parameters for controllers.

PI parameter	Vk_p	Vk_i	Ik_p	Ik_i
Lower bound	0.00	2000.00	10.00	63.25
Upper bound	2.00	3000.00	25.00	63.30

Fig. 6 illustrates the flowchart process of the PSO algorithm, depicting the sequential steps involved in optimizing the parameters to achieve the desired outcome.

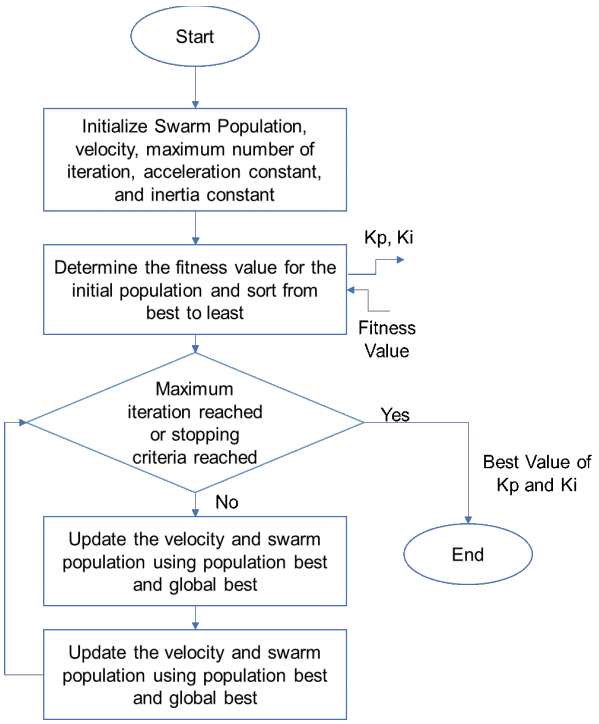

Fig 6. Flowchart of PSO algorithm.

The dynamic model created through the Laplace transform of the mathematical model used the PSO algorithm as the objective function. Typically, PSO is known as a non-model-based controller. However, in

this research, PSO was employed as an offline tuner for the double-loop PI controller, necessitating an understanding of the entire inverter system's dynamics. The PSO algorithm was implemented in a MATLAB syntax script by setting specific parameters such as the number of swarm populations, number of iterations, and number of variables. The gain parameters for both controllers were determined by the algorithm and utilized as the PI controllers' parameters. The dynamic model of the entire inverter system in Eq. (5) employed a step signal as a reference, with the determined controller parameters expressed in Eq. (6).

$$\frac{V_o(s)}{1/s} = \frac{0.01429s^4+151.8s^3+407.8s^2}{(2.993\times10^{-12})s^6+(3.261\times10^{-7})s^5+0.1429s^4+151.8s^3+407.8s^2} \quad (6)$$

2.3 Fuzzy logic implementation

Fuzzy logic controller enables the PSO-PI parameters to be tuned according to the expert analysis. Even more helpful that fuzzy logic tunes the parameters through online tuning approached where the value of the controller parameter may change according to the system stability and performance in a particular time frame. Fuzzy logic was implemented by utilizing the error of the output voltage 'e' and the rate of change of error 'ec' as inputs, as depicted in Fig. 7. Fuzzy logic was integrated into both voltage controllers and current controllers, with the PI parameters optimized by the PSO algorithm.

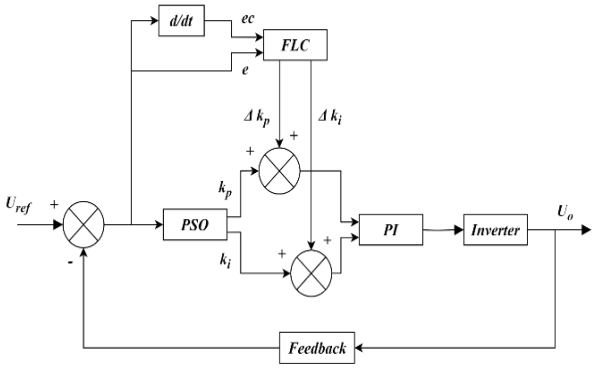

Fig 7. Fuzzy logic controller structure.

The input of the FLC, as previously mentioned, includes the e and the ec, while the outputs comprise changes of Δk_p and Δk_i. This setup is implemented in both the voltage controller and current controller. The domain of input and output variables is partitioned into three sections: Negative (N), Zero (Z), and Positive (P). The membership function is a combination of Gaussian and triangle function, illustrated in Fig. 8 and Fig. 9.

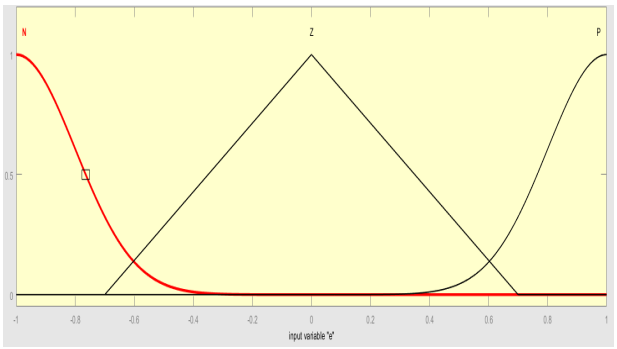

Fig 8. Membership function of error.

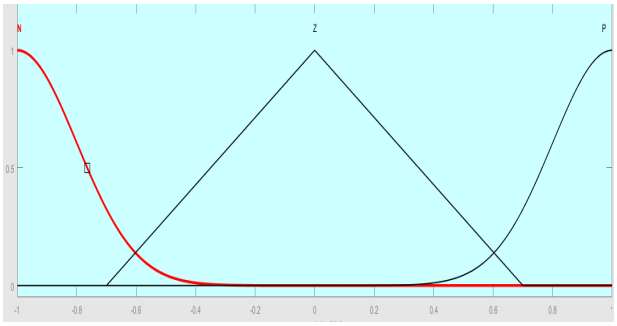

Fig 9. Membership function for change of K_P.

The membership function value is determined by using fuzzy rules during the fuzzification process. The fuzzy rules are derived from the observing the system's stability, steady-state, time response and overshoot. Through this process, the value of Δk_p and Δk_i for both voltage controller and current controller are established. These fuzzy rules are documented in Table 4 and Table 5. The e and ec for voltage and current parameters are input into their respective FLC domains.

Table 4. Fuzzy rules for Δk_p.

e \ ec	N	Z	P
N	N	N	N
Z	N	P	P
P	P	P	P

Table 5. Fuzzy rules for Δk_i.

e \ ec	N	Z	P
N	Z	Z	Z
Z	P	P	P
P	Z	Z	Z

These membership functions play a crucial role in determining the values after the fuzzification and

defuzzification processes. Before proceeding, the process must undergo rule evaluation based on rules provided by the expert system. The membership function is categorized into three levels for both inputs and outputs: negative (N), zero (Z), and positive (P). Gaussian membership function represents the N and P levels, while triangle membership function is used for the Z level. These three levels signify the degree of the values for inputs and outputs, which are compared during rule evaluation. The rules are established considered system stability, steady-state, time response and overshoot, requiring adjustments to the values of K_p and K_i. The flowchart of fuzzy logic process is illustrated in Fig. 10. All the PI controller parameters optimized by their respective optimization are tabulated in Table 6.

Table 6. All PI controller parameters.

	PSO-PI		FLC-PSO-PI	
Controller	k_p	k_i	k_p	k_i
Voltage (V)	0.2056	2182.20	0.2056 ± 0.1	2182.20 ± 100
Current (I)	23.5395	63.2702	23.5395 ± 2	63.2702 ± 10

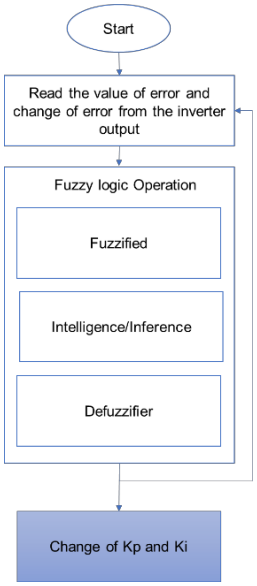

Fig 10. Flowchart of FLC.

3 Results

3.1 Output waveform of transient analysis

The output waveform of transient analysis provides crucial insights into the dynamic behaviour of MLI under varying load conditions. By examining the response of the circuit over time, particularly during the transition from one steady state to another, we can identify key characteristics such as overshoot, undershoot, rise time and settling time.

- **Half load to full load**

The half load to full load condition was utilized in this research to observe the transition from 50 % of the rated load to its maximum load. This transition occurs during breaker trips to enable current flow through the designated load of 30 Ω. In this scenario, the switching can be viewed as disturbance to the steady state as the system transitions from half load to full load condition. The analysis focuses on the transient response duration required to achieve a steady state during full load condition under a sinusoidal signal. Fig. 11 displays the output waveform during the half load to full load condition when the FLC-PSO-PI controller is applied.

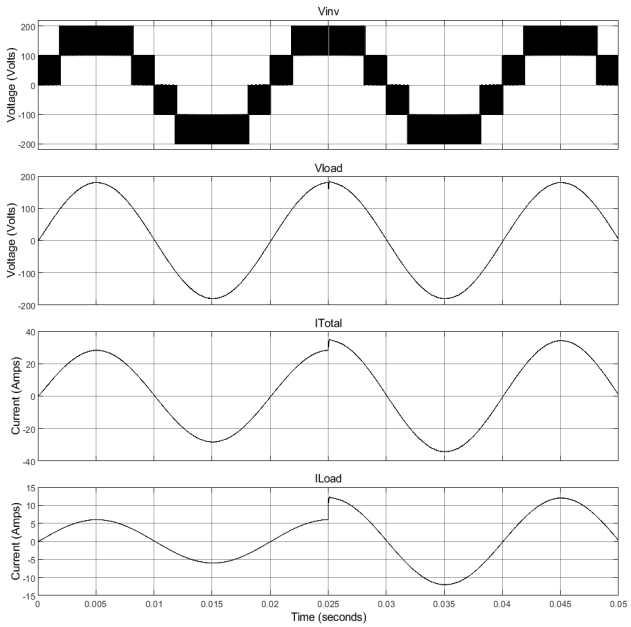

Fig 11. Output waveform of half load to full load using FLC-PSO-PI controller.

The output voltage for FLC-PSO-PI controller that was the focus during the switching transition is depicted in Fig. 12.

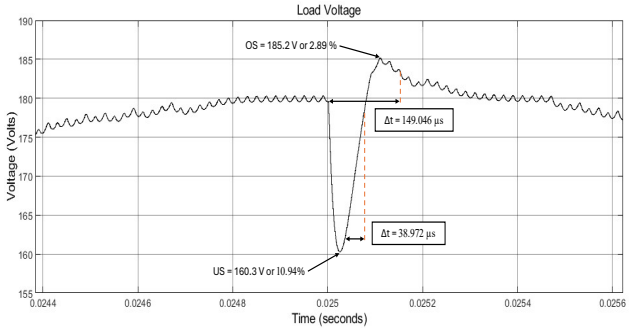

Fig 12. Switching duration of output voltage.

The FLC-PSO-PI using a settling time of 149.046 µs to return the switching transition of output voltage back to it 2 % of steady state and a rise time of 38.972 µs for the

voltage to climb up to it 10 % of lower and upper threshold voltage, showcasing an improvement over PSO-PI and no controller (NC). In addition, the overshoot during transient phase is 2.89 % which is lower than PSO-PI and NC with falls within permissible limits for general rating, ensuring it does not exceed the peak voltage of 200 V before considering the modulation index. This controller fails to meet the desired voltage drop limit during switching and causes a dramatic fall of undershoot with listed 10.94 %.

3.2 Voltage output analysis

The voltage output analysis focuses on the comprehensive examination of the sinusoidal waveform of the output voltage. The analysis encompasses the impact on the peak voltage value and THD of the voltage waveform in NC, PSO-PI and FLC-PSO-PI controller. The NC output is used as the baseline of performance of other controllers. The results for the output voltage analysis the half load to full load condition and the no load to full load condition.

- **Half load to full load**

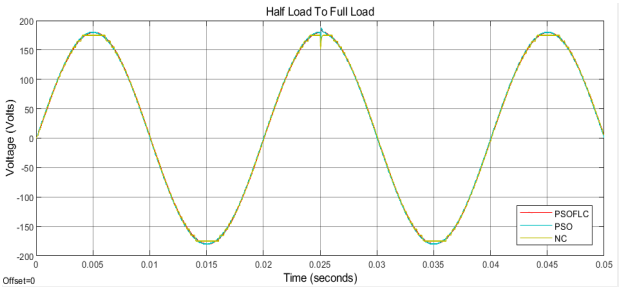

Fig 13. Output voltage waveform of half load to full load with different controllers.

Fig. 13 shows the comparison of output voltage waveform under half load to full load conditions. The waveform represented NC, PSO-PI, and FLC-PSO-PI are used for the inverter. The results indicate that all types of controllers successfully achieve the goal of generating a smooth AC waveform. However, the inverter without controller fails to generate a complete smooth sinusoidal of an AC waveform and the waveform is more likely as staircase. The THD value recorded for each controller serves as evidence of how well the controller maintains the output voltage waveform closer to the ideal fundamental shape but without controller will be difficult to maintain the output voltage waveform.

In Fig. 14, the transition from half load to full load occurs within 0.025 s in the NC, PSO-PI and FLC-PSO-PI. The no controller drawn a lowest undershoot pattern and the PSO-PI drawn a highest overshoot pattern. However, neither controllers fail to maintain a low undershoot level nor voltage drop level.

Overall, the FLC-PSO-PI drawn an optimum waveform compared to others.

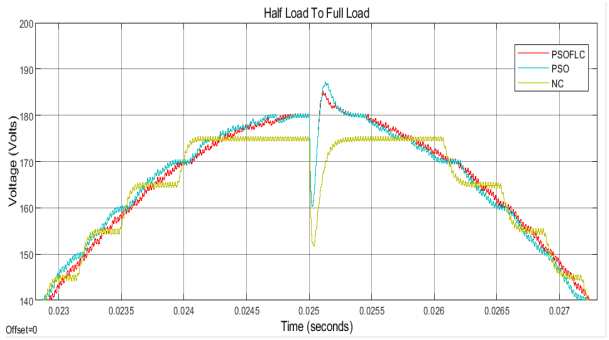

Fig 14. Rectified voltage comparison with different controllers.

- **No load to full load**

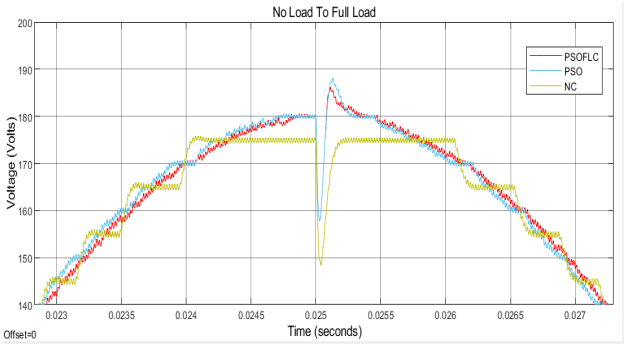

Fig 15. Switching characteristic comparison with different controllers.

In Fig. 15, the transition from no load to full load occurs within 0.025 s in the NC, PSO-PI and FLC-PSO-PI. The no controller drawn a slightest undershoot pattern and the PSO-PI drawn a greatest overshoot pattern. However, all controllers also fail to maintain a low undershoot level or voltage drop level.

4 Discussion

4.1 Transient analysis

Transient analysis involves assessing the time required for the system to stabilize the output voltage during disturbances. Specifically, in this context, the voltage drops resulting from switching actions serves as a disturbance for the system. The analysis includes time trend and rate of overshooting observed at 0.025 s during switching. The analysis encompasses evaluating parameters such as overshoot, rise time, and settling time of the multilevel inverter system for the analysis from half load to full load and no load to full load.

- **Rise time**

The rise time indicate the time taken for the output voltage signal to cross a 10 % of lower and upper

threshold voltage. Fig. 16 shows a bar graph of rising time using different type of controllers.

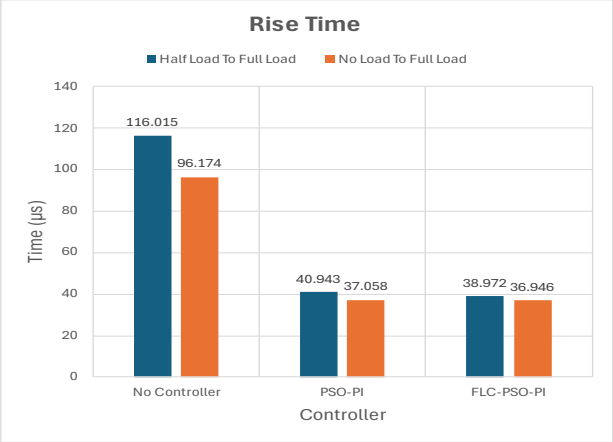

Fig 16. Rise time for half and no load to full load.

The PSO-PI and FLC-PSO-PI controllers exhibit faster rise time than the system with no controller, indicating that both controllers has more responsive system to feedback. The half load to full load condition consumes a lot of time to overcome the switching transition compared to no load to full load in all controllers. This represent that half load to full load have a slow responsive system to load. The inverter without controller rising time is almost triple of MLI that contain controller. This meaning that controller can help the MLI to shorten then voltage climbing period to recover the voltage rapidly.

- **Overshoot and settling time**

In control system, overshoot is how much of the peak voltage produced by controller exceeds the targeted voltage. In half load to full load, the percentages of overshoot for PSO-PI and FLC-PSO-PI controllers are 3.94 % and 2.89 %, respectively, while no load to full load are 4.11 % and 3.44 %, respectively. All of them are below 10 % of voltage drop which are acceptable in electrical system. The difference of load is half, but the overshoot is not the half. The NC did not happen any overshoot during switching.

The settling time is the time needed for the controller to reach the steady state and stay within the 2 % of tolerance bands around the targeted voltage. The inverter without controller of settling time is faster than with controller. The characteristics of the recorded data for the transient analysis during the transition from half and no load to full load are summarized in Table 7. The table indicates that the overshoot produced by the system affected the settling time, which refers to the duration for the system achieves stable voltage fluctuations.

Table 7. Overshoot and settling time for half and no load to full load.

Controller	Overshoot (%)		Settling Time (µs)	
	Half load to full load	No load to full load	Half load to full load	No load to full load
NC	0.00	0.00	147.040	136.963
PSO-PI	3.94	4.11	190.968	166.426
FLC-PSO-PI	2.89	3.44	149.046	151.014

Overall, the FLC-PSO-PI controller prove as the fastest controller in giving feedback which is needed in this load condition since the voltage drop happen during switching is quite critical for all controller type.

4.2 Voltage of output analysis

Output voltage analysis involves a comprehensive of the sinusoidal waveform of the output voltage, assessing parameters such as peak voltage and THD of the voltage waveform. The results of the output voltage analysis during half and no load to full load condition.

- **Total harmonic distortion**

The THD is a measurement of the distortion of a voltage is due to harmonic in the output voltage AC signal cause by the controller. Fig. 17 shows bar graph of THD using different type of controllers and different load. The NC exhibits the highest THD value compared to other controllers, with FLC-PSO-PI controller ranking second in THD improvement. Notably, PSO-PI controller effectively reduces THD during the switching process, with a slight greater than 0.1 % difference compared to FLC-PSO-PI controller. The MLI starting with no load is marginally higher than starting with half load in all case.

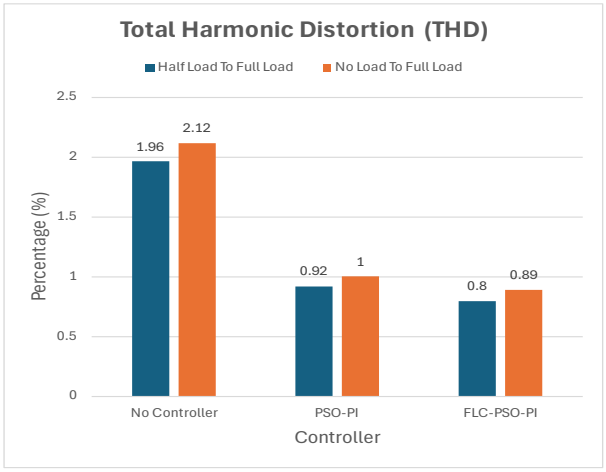

Fig 17. THD for half and no load to full load.

- **Voltage drop and undershoot**

The analysis results with a half load mirror those of the no load scenario, without controller achieving an average peak voltage of 175 V, while PSO-PI and FLC-PSO-PI controllers maintain a consistent peak voltage of 180 V for both half and no load to full load condition. Table 8 shows the voltage drop and undershoot for half and no load to full load using with and without controller.

Table 8. Voltage drop and undershoot for half and no load to full load.

Controller	Voltage Drop during Switching (V)		Undershoot / Voltage Drop Level (%)	
	Half load to full load	No load to full load	Half load to full load	No load to full load
NC	22.81	26.1	13.31	15.20
PSO-PI	19.28	21.71	10.94	12.28
FLC-PSO-PI	19.28	21.71	10.94	12.28

The voltage drops during switching for NC in both half and no load to full load condition listed the lowest voltage drop value as 22.81 V and 26.1 V, respectively. However, the PSO-PI and FLC-PSO-PI capable to minimize the voltage drop at the same level where half load to full load is 19.28 V and no load to full load is 21.71 V.

Besides that, undershoot is a percentage of the voltage fall exceeding the targeted voltage. The no controller for transition in half load to full load is 13.31 % and no load to full load is 15.20 %. The PSO-PI and FLC-PSO-PI shows lower undershoot percentage where half load to full load is 10.94 % and no load to full load is 12.28 %. Despite all of them failing to meet the desired undershoot limit during switching. This drop is attributed to physical switching rather than system instability. The use of a running capacitor at the load can significantly mitigate this effect. Furthermore, there is an observable improvement when using PSO-PI and FLC-PSO-PI controller compared to no controller. This highlights how controllers can mitigate the voltage drop effect cause by physical switching processes.

5 Conclusions

Based on the provided sources, the PSO algorithm plays a significant role in enhancing the determination of PI controller parameters. When FLC combined with PSO algorithm and PI controller to form a FLC-PSO-PI controller, this integration proves to be a superior choice. The PSO algorithm optimize the PI controller parameters accurately and effectively, while the fuzzy logic component acts as an online tuner, particularly when the MLI introduces changes in half load and no load to full load effects. The proposed technique demonstrates outstanding performance across different load scenarios, effectively reducing voltage output error and ensuring high-quality transient responses.

Conflict of Interest

The authors declare no conflict of interest.

Acknowledgment

This work was supported in part by the Ministry of Higher Education of Malaysia under the Translational Research Grant no RDU233602 and in part of Tabung Persidangan Dalam Negara (TPDN) Universiti Malaysia Pahang Al-Sultan Abdullah.

References

[1] A. Akbari, J. Ebrahimi, Y. Jafarian, and A. Bakhshai, 'A multilevel inverter topology with an improved reliability and a reduced number of components', *IEEE J Emerg Sel Top Power Electron*, vol. 10, no. 1, pp. 553–563, Feb. 2022, doi: 10.1109/JESTPE.2021.3089867.

[2] G. K. Srinivasan, M. Rivera, V. Loganathan, D. Ravikumar, and B. Mohan, 'Trends and challenges in multi-level inverter with reduced switches', *Electronics 2021, Vol. 10, Page 368*, vol. 10, no. 4, p. 368, Feb. 2021, doi: 10.3390/ELECTRONICS10040368.

[3] A. Lewicki, C. Odeh, and M. Morawiec, 'Space vector pulsewidth modulation strategy for multilevel cascaded h-bridge inverter with dc-link voltage balancing ability', *IEEE Transactions on Industrial Electronics*, vol. 70, no. 2, pp. 1161–1170, Feb. 2023, doi: 10.1109/TIE.2022.3158005.

[4] S. Hayat, S. S. Syed, S. S. Syed, S. Shabbir, and J. Khan, '63-level reduce switch asymmetrical cascaded h-bridge multilevel inverter', *2020 IEEE 23rd International Multitopic Conference (INMIC)*, Nov. 2020, doi: 10.1109/INMIC50486.2020.9318100.

[5] S. K. Chien, S. Y. Sim, W. M. Utomo, S. L. Kek F. Mustafa, N. A. Zambri, A. J. L M. Siang and G. Y. Sim, 'Enhanced DTC induction motor drives for THD minimization performance improvement with multilevel inverter', *International Journal of Power Electronics and Drive Systems (IJPEDS)*, vol. 13, no. 1, pp. 93–101, Mar. 2022, doi: 10.11591/IJPEDS.V13.I1.PP93-101.

[6] B. Mahato, S. Majumdar, K. C. Jana, A. Agrawal, and A. Shrivastava, 'A generalized series-connected multilevel inverter (MLI) based on reduced power electronic devices for symmetrical/asymmetrical sources', *Arab J Sci Eng*, vol. 48, no. 5, pp. 5907–

5924, May 2023, doi: 10.1007/s13369-022-07066-z.

[7] R. Gadal, A. Oukennou, F. El Mariami, A. Belfqih, and N. Agouzoul, 'Voltage stability assessment and control using indices and FACTS: A comparative review', *Journal of Electrical and Computer Engineering*, vol. 2023, no. 1, p. 5419372, Jan. 2023, doi: 10.1155/2023/5419372.

[8] H. S. Salama and I. Vokony, 'Voltage stability indices–A comparison and a review', *Computers & Electrical Engineering*, vol. 98, p. 107743, Mar. 2022, doi: 10.1016/J.COMPELECENG.2022.107743.

[9] S. K. Sadula, R. Challoo, X. Fu, and S. Li, 'Novel cost-effective technique for continued operation of electrical equipment during voltage sag', *International Journal of Engineering (IJE)*, vol. 13, no. 1, pp. 1–36, 2021.

[10] IEEE, 'IEEE standard for harmonic control in electric power systems', *ANSI/IEEE Std. 519*, vol. 2022, p. 17, Aug. 2022, doi: 10.1109/IEEESTD.2022.9848440.

[11] IEC, 'IEC standard voltages', *IEC 60038:2009+AMD1:2021 CSV Consolidated version*, 2021.

[12] H. Katir, A. Abouloifa, E. Elbouchikhi, A. Fekih, K. Noussi, and A. El Aroudi, 'Robust control of cascaded h-bridge multilevel inverters for grid-tied PV systems subject to faulty conditions', *IEEE Control Syst Lett*, vol. 7, pp. 2683–2688, 2023, doi: 10.1109/LCSYS.2023.3288494.

[13] J. H. Urrea-Quintero, J. N. Fuhg, M. Marino, and A. Fau, 'PI/PID controller stabilizing sets of uncertain nonlinear systems: an efficient surrogate model-based approach', *Nonlinear Dyn*, vol. 105, no. 1, pp. 277–299, Jul. 2021, doi: 10.1007/S11071-021-06431-1/FIGURES/15.

[14] S. Ab-Ghani, H. Daniyal, A. Z. Ahmad, N. Jaalam, N. M. Saad, N. H. Ramlan and N. Bahari, 'Adaptive online auto-tuning using particle swarm optimized PI controller with time-variant approach for high accuracy and speed in Dual Active Bridge converter', *AIMS Electronics and Electrical Engineering*, vol. 7, no. 2, pp. 156–170, 2023, doi: 10.3934/electreng.2023009.

[15] S. Ab-Ghani, H. Daniyal, N. Jaalam, N. M. Saad, and N. H. Ramlan, 'Dynamic control and performance of dual active bridge converter based particle swarm optimization', *IET Conference Proceedings*, vol. 2022, no. 22, pp. 312–316, 2022, doi: 10.1049/ICP.2022.2633.

[16] S. Ab-Ghani, H. Daniyal, N. H. Ramlan, and M. C. Tiong, 'Online PSO-tuned phase shift angle controller for dual active bridge DC–DC converter', *SN Appl Sci*, vol. 2, no. 1, pp. 1–8, Jan. 2020, doi: 10.1007/S42452-019-1782-8/TABLES/4.

[17] M.Izzat Nordin, Leong Ying Foo, M.H.A. Ab Malek, Suliana Ab Ghani, and N.Huda Ramlan, 'Performance analysis of reduced switch hybrid cascaded multilevel inverter with PSO-based PI controller during load variations', *Proceedings of International Exchange and Innovation Conference on Engineering & Sciences (IEICES)*, vol. 10, pp. 874–881, Oct. 2024, doi: 10.5109/7323363.

[18] A. Tamer, L. Zellouma, M. T. Benchouia, and A. Krama, 'Adaptive linear neuron control of three-phase shunt active power filter with anti-windup PI controller optimized by particle swarm optimization', *Computers & Electrical Engineering*, vol. 96, p. 107471, Dec. 2021, doi: 10.1016/J.COMPELECENG.2021.107471.

[19] C. Sain, A. Banerjee, P. K. Biswas, T. S. Babu, and T. Dragicevic, 'Updated PSO optimised fuzzy-PI controlled buck type multi-phase inverter-based PMSM drive with an over-current protection scheme', *IET Electr Power Appl*, vol. 14, no. 12, pp. 2331–2339, Dec. 2020, doi: 10.1049/IET-EPA.2020.0165.

[20] A. Bouchakour, A. Borni, and M. Brahami, 'Comparative study of P&O-PI and fuzzy-PI MPPT controllers and their optimisation using GA and PSO for photovoltaic water pumping systems', *International Journal of Ambient Energy*, vol. 42, no. 15, pp. 1746–1757, Nov. 2021, doi: 10.1080/01430750.2019.1614988.

[21] R. Kumar, 'Fuzzy particle swarm optimization control algorithm implementation in photovoltaic integrated shunt active power filter for power quality improvement using hardware-in-the-loop', *Sustainable Energy Technologies and Assessments*, vol. 50, p. 101820, Mar. 2022, doi: 10.1016/J.SETA.2021.101820.

[22] J. Siahbalaee and N. Sanaie, 'Comparison of conventional and new cascaded multilevel inverter topologies based on novel indices', *ISA Trans*, vol. 119, pp. 41–51, Jan. 2022, doi: 10.1016/J.ISATRA.2021.02.025.

Biographies

Mr. Ying Foo Leong received the B.Eng. (Hons.) degree in electrical engineering (power systems) from Universiti Malaysia Pahang Al-Sultan Abdullah, Malaysia, in 2024. He is currently working toward the Ph.D. degree in electrical engineering at Universiti Malaysia Pahang Al-Sultan Abdullah, Malaysia. His research field includes multilevel inverter, power electronics, renewable energy, artificial intelligence, and energy management.

Mr. Nizaruddin M.Nasir received the B.Eng. (Hons.) degree in electrical engineering (power systems) from Universiti Malaysia Pahang Al-Sultan Abdullah, Malaysia, in 2023. He is currently working toward the Ph.D. degree in electrical engineering at Universiti Malaysia Pahang Al-Sultan Abdullah, Malaysia. His research field includes power electronics, artificial intelligence and energy management.

Dr. Suliana Ab-Ghani received the M.Sc. degree in electrical engineering from Universiti Teknologi Malaysia, Malaysia, in 2010 and the Ph.D. degree in electrical engineering from Universiti Malaysia Pahang Al-Sultan Abdullah, Malaysia, in 2021. Her main research interests include dual active bridge, power electronics and particle swarm optimization.

Dr. Norazila Jaalam received the B.Eng. degree in electrical engineering (electronics) from Universiti Malaysia Pahang Al-Sultan Abdullah, Malaysia, in 2006, and the M.Sc. degree in electrical power from Newcastle University, United Kingdom, in 2008, and the Ph.D. degree in electrical engineering from Universiti Malaya, Malaysia, in 2022. Her research field includes power electronics, renewable energy, artificial intelligence and energy management.

Dr. Nur Huda Ramlan received the B.Eng. degree in electrical and electronics (power systems) from Universiti Teknologi PETRONAS, Malaysia, in 2009, and the M.Sc. degree in electrical power and the Ph.D. degree in electrical engineering from the Universiti Teknologi Malaysia, Malaysia, in 2011 and 2017, respectively. Her main research interests include multilevel inverter and controller.